$$\alpha_O = \frac{2\pi^2\lambda_O f_O f^2}{\rho c^3(f_O + f^2/f_O)}, \qquad \alpha_N = \frac{2\pi^2\lambda_N f_N f^2}{\rho c^3(f_N + f^2/f_N)} \tag{22}$$

Comparing Eq. (22) with Eq. (6) one gets the relaxation viscosities of oxygen and nitrogen λ_O and λ_N in the air.

$$\lambda_O = \frac{\rho c^3 G_O}{2\pi^2 f_O}, \qquad \lambda_N = \frac{\rho c^3 G_N}{2\pi^2 f_N} \tag{23}$$

In Table 1 the numerical values λ_O and λ_N of the standard atmosphere calculated with Eqs. (7), (8), and (23) are given.

V. Approximated Flow Equation in Air

As an alternative to the exact solution of Eq. (18), the convolution integrals may be substituted by Taylor series expansions with

$$v(t-t^*) = \sum_{n=0} \frac{1}{n!}\frac{d^n v}{dt^n}(-t^*)^n = v - \left(\frac{\partial v}{\partial t} + v\nabla v\right)t^* \pm \quad \ldots \tag{24}$$

The flow equation in air is as follows:

$$\frac{\rho\partial v}{\partial t} + \rho v \cdot \nabla v = -\text{grad}\, p + \eta\left(\nabla v + \frac{1}{3}\text{grad div } v\right) + \mu\,\text{grad div } v + \lambda_O\,\text{grad div} \sum_{n=0}\left(\frac{-1}{2\pi f_O}\right)^n \frac{d^n v}{dt^n} + \lambda_N\,\text{grad div} \sum_{n=0}\left(\frac{-1}{2\pi f_N}\right)^n \frac{d^n v}{dt^n} \tag{25}$$

For air flow under environmental conditions, the zeroth-order term $n = 0$ may be sufficient. For normal air humidity values, the relaxation frequencies are well separated; for nitrogen, f_N = 100–300 Hz, whereas for oxygen, f_O = 20,000–30,000 Hz. Defining the Strouhal numbers St_N and St_O with d_c the characteristic length and v_c the characteristic velocity

$$St_N = f_N d_c/v_c, \qquad St_O = f_O d_c/v_c \tag{26}$$

For flow velocities with a Strouhal number $St = fd_c/v_c$ the flow equation (25) can be approximated by

$$\frac{\rho\partial v}{\partial t} + \rho v \cdot \nabla v = -\text{grad}\, p + \eta\Delta v + \begin{Bmatrix} (1/3)\eta + \mu + \lambda_O + \lambda_N \\ (1/3)\eta + \mu + \lambda_O \\ (1/3)\eta + \mu \end{Bmatrix} \text{grad div } v$$

$$\text{for} \begin{Bmatrix} St < St_N \\ St_N < St < St_O \\ St > St_O \end{Bmatrix} \tag{27}$$

In the standard atmosphere at sea level the shear viscosity is $\eta = 1.7 \times 10^{-5}$ kg/ms, and the relaxation viscosity of atmospheric oxygen $\lambda_O = 4.6 \times 10^{-4}$ kg/ms. In this case the term grad div v is 79.2 times higher than in the classical Navier-Stokes equation without the vibrational relaxation effect.

References

[1]Knudsen, V. O., "The Absorption of Sound in Air, in Oxygen, and in Nitrogen—Effects of Humidity and Termperature," *Journal of the Acoustical Society of America*, Vol. 5, Oct. 1933, pp. 112–121.

[2]Kneser, V. O., "The Interpretation of the Anomalous Sound-Absorption in Air and Oxygen in Terms of Molecular Collisions," *Journal of the Acoustical Society of America*, Vol. 5, Oct. 1933, pp. 122–132.

[3]Greenspan, M., "Rotational Relaxation in Nitrogen, Oxygen, and Air," *Journal of the Acoustical Society of America*, Vol. 31, 1959, pp. 155–160.

[4]Pierce, A. D., *Acoustics*, McGraw-Hill, New York, 1989, pp. 508–565.

[5]Thompson, P. A, *Compressible-Fluid Dynamics*, McGraw-Hill, New York, 1972.

[6]Anon., "Acoustics-Attenuation of Sound During Propagation Outdoors," Pts. 1 & 2, International Standard Organization, ISO/TC 43/SC 1/WG 24, Central Secretariat, CH-1211 Geneva 20, Switzerland, Aug. 1988.

Time-Of-Flight Mass Spectrometer for Impulse Facilities

K. A. Skinner* and R. J. Stalker†
University of Queensland, St. Luica 4072, Australia

Introduction

At present, impulse facilities such as shock tunnels and expansion tubes are the only practical ground-based means of simulating aerodynamic conditions at speeds in excess of 3.5 km/s. The duration of test flow, however, is of the order of a millisecond, requiring specialized instrumentation. It is especially desirable to measure species concentrations in the test flow since the chemical state of the test gas may be altered by the high transient temperatures produced. Also, the flow of test gas in a reflected shock tunnel is followed by a flow of driver gas, usually of a different composition. The breakdown of the interface between these two gas slugs causing mixing of the driver and test gases typically limits the available test time. Measurements of species concentrations are the most sensitive methods of determining the duration of test flow and have been used in the past.[1] Furthermore, studies of supersonic combustion ramjets would benefit from measurements of species concentrations downstream of fuel injection.

A quadrupole mass spectrometer was used by Crane and Stalker[2] in a reflected shock tunnel. They used a two-stage hollow conical skimmer gas sampling system. The short duration of the flow meant that the ions from only a single species of molecule could be recorded during each test flow. To obtain relative concentrations, Crane and Stalker relied upon sampling multiple test flows and measured the total ion production of each shot for normalization. This method assumed repeatability of the test flow and of the behavior of the mass spectrometer despite variations in total ion production. They estimated errors in their relative species concentration measurements of 30%.

Experimental Design

The instrument reported here was designed for use in T4, an existing free piston reflected shock tunnel.[3] At the upstream end are three coaxial, hollow conical skimmers used to sample the flow (Fig. 1). Behind the second and third skimmers are vacuum chambers evacuated by diffusion pumps. There is no vacuum chamber behind the first skimmer as the flow through it vents back out into the freestream flow. Gas passing through the skimmers is expanded and collimated into a molecular beam entering the interior high vacuum chamber. At 20 mm behind the final skimmer, an electron beam intersects the molecular beam, causing ionization of some molecules. The ions produced are accelerated along a meter-long flight tube to an electron multiplier particle detector. The signal from this particle detector is recorded on a digital storage oscilloscope.

An essential aspect of the success of the instrument is that the production of the molecular beam be achieved as quickly as possi-

Received Feb. 6, 1993; revision received March 8, 1994; accepted for publication March 21, 1994.

*Research Student, Department of Mechanical Engineering. Member AIAA.

†Professor of Space Engineering, Department of Mechanical Engineering. Member AIAA.

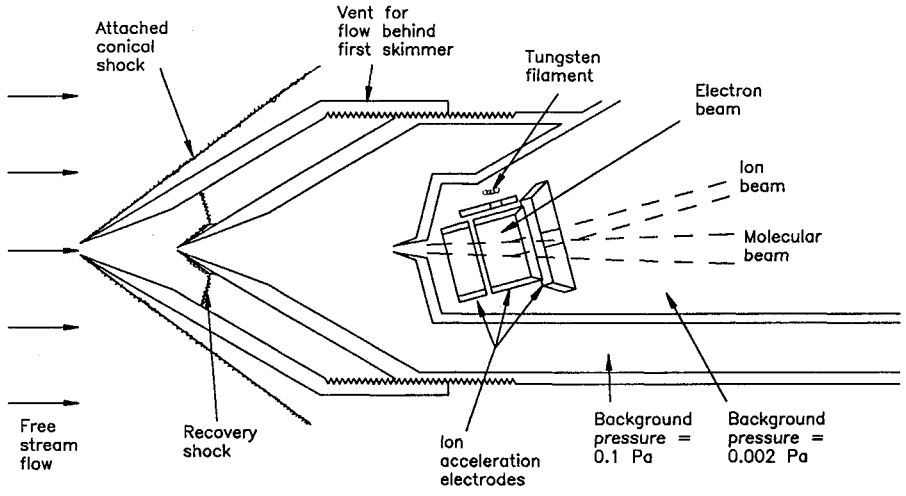

Fig. 1 Schematic of skimmer configuration and ionization region.

ble. The front skimmer served to both decrease the density and increase the Mach number of the flow entering the second skimmer. The density of the flow falls by an order of magnitude in 5 mm (or 1 μs). The second skimmer samples this expanded flow on the axis. Off-axis flow passes around the second skimmer experiencing a normal shock recovery of pressure to a stagnation pressure higher than the freestream static pressure. This flow can then vent back out into the freestream. For an incident Mach number of 5.5, the recovery shock Mach number is at least 10.8 for a ratio of specific heats from 1.3 to 1.4. The maximum interskimmer distance was then found from a method of characteristics calculation. This gave the density at the second skimmer as 0.03 times the freestream density. To produce the fastest possible expansion, the orifice diameter of the second skimmer was chosen to be as small as practicably manufacturable (0.7 mm). The third skimmer collimates the flow 40 mm behind the second skimmer. Approximate calculations give the density in the molecular beam as 0.0001 times the freestream density. For a freestream test flow of air at 0.05 kg/m^3 and an enthalpy of 9 MJ/kg, the expansion through the skimmers results in a molecular beam density of 5×10^{-6} kg/m^3, or a flux of 10^{23} particles/m^2/s. The flow is chemically frozen during the expansion inside the first skimmer; and estimates give that the average molecule experiences less than 70 collisions before reaching the ionizer. The production of this beam is achieved in a distance of 75 mm with an external diameter of the skimmers of only 50 mm. This is small enough to allow the probe access to complex flowfields such as scramjet nozzles, a region inaccessible to optical methods of species measurement.

Extraction of gas samples by forming a molecular beam from a continuum flow is a technique developed in the 1950–1960s.[4–6] Ideally, the axial stream tube experiences no disturbance other than the strong expansions inside each skimmer. In practice, as the flow expands from continuum to free molecular, there is interference from flow particles reflecting off the outside (for large half-angles) or the interior (for small half-angles) of the skimmer. These particles can penetrate the beam and scatter the undisturbed particles. Bird[7] examined the effect of Knudsen number and skimmer geometry on molecular beam interference using a Monte-Carlo simulation and concluded that with correct design the interference can be negligible. Correct design consists of short skimmers, a lip radius much less than the orifice diameter, and a Knudsen number based on orifice diameter outside the range of 0.1–2. The Knudsen number at the third skimmer is approximately 50, and the length of the skimmer is less than half the length of that studied by Bird. Very little interference from the third skimmer was expected.

A further influence on the sample is that an expansion of a mixture of gases to free molecular flow can cause a relative depletion of lighter particles on the axis. Sebacher[8] and Sherman[9] suggest that diffusion in the strong pressure gradients near the start of the expansion inside the skimmer is the mechanism responsible. The work of Fenn and Anderson[10] indicates scattering from background molecules penetrating the flow after the beam has translationally frozen as the cause. Either explanation allows for a variation with mass ratio; the latter allows for an additional variation with molecular diameter. Whatever the physical situation, the state of knowledge about the process is not sufficient to make purely theoretical corrections to species concentrations, and thus calibration is required to account for its effect.

Mass Separation

Separation of different mass components of the sample molecular beam is achieved with an ion time-of-flight system.[11] A pulsed electron beam intersects the molecular beam 20 mm behind the third skimmer. This region is held at a potential above ground by a surrounding cylindrical electrode coaxial with the drift tube. The potential gradient within the intersection region is set by adjacent coaxial electrodes at the either end (Fig. 1). The electron beam is formed by accelerating electrons emitted from a 6-W tungsten filament through a gate electrode, through a 2-mm-diam hole in the side of the central cylindrical electrode. The electron gun can be pulsed on for 200 ns, producing a beam of 1 mA. The ions are formed at a potential of 250 V in a field gradient of 20 V/mm.

After ionization, the ions are accelerated down a potential field gradient to a field-free drift region 1 m long. The flight time t along this region depends on the mass simply as

$$t = L\sqrt{\frac{m}{2qE}}$$

where L is the length of the drift region, m/q the mass to charge ratio, and E the energy given to the ion. The electron gun was pulsed on for 200 ns every 0.055 ms producing a packet of ions which were then detected and recorded on a storage oscilloscope. The oscilloscope sampled the signal at 10 MHz for 6.4 ms, allowing 117 complete spectra to be obtained during each firing of the shock tunnel. The limiting resolution is determined by the sampling rate of the data storage, the degree to which the peaks spread at higher mass numbers because of their energy spread, and the spread in peak width due to collisions with background molecules.

Calibration

From the freestream values, the concentrations of the species present are altered by the measurement process in three ways that require calibration. First is the possibility of light molecule depletion on the axis of the expansion inside the skimmers. This can be incorporated into measurements as a relative calibration factor F. Second, in the molecular beam, the relative number of ions formed for each species is proportional to their ionization cross section σ.

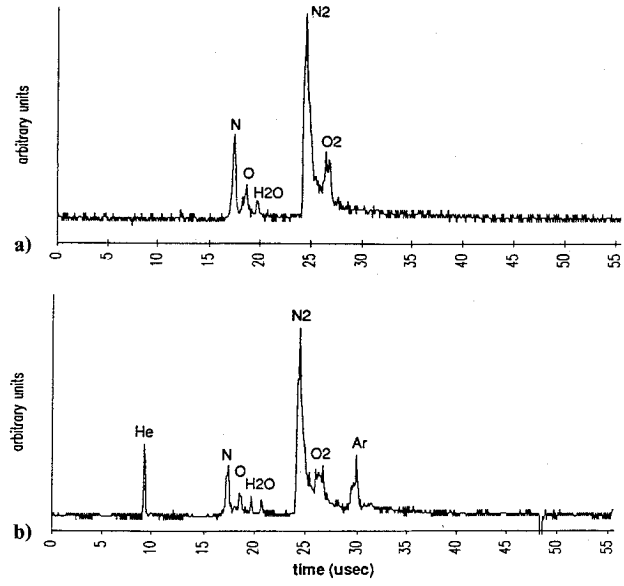

Fig. 2 Sample spectra recorded during a flow with air test gas: a) spectra during test time and b) spectra later in time showing arrival of driver gas.

Finally, the efficiency of collection of ions by the detector of each species may vary. Again, the concentrations can be related by a constant calibration factor C provided external effects such as vacuum level and acceleration potentials are held constant.

Thus, all effects on the sample are proportional effects, and a single calibration factor is sufficient to describe them all. However, where F and C are not unity, calibration of the mass spectrometer using known gas mixtures must be performed. Calibration factors were obtained for mixtures of He-N_2, H_2-N_2, and Ar-N_2. For molecules of very similar mass and size (for example, N_2, NO, and O_2), F and C can both be taken to be unity. Ionization cross sections are available in the literature.

For a diatomic molecule, dissociative ionization produces atomic species, even when there are none in the test flow. Thus, N_2 and O_2 molecules produce N and O atoms under electron impact ionization. Fortunately, this is taken into account in the collision cross sections, so the effect can be ignored when determining molecular species.

Performance

The mass spectrometer has been used in 147 test flows of a free-piston reflected shock tunnel. Of these approximately 70% produced useful results. Figure 2 shows an early result, consisting of two of the 117 mass spectra from air test gas at an enthalpy of 9 MJ/kg. The graph of Fig. 2a was taken during test time, and that of Fig. 2b when the flow was contaminated by driver gas. Peak separation is good except for the N_2, NO, O_2 peaks. These are thought to overlap because collisions with background molecules within the drift region cause loss of energy from some ions, spreading the tail of the peak. This can be remedied by reducing the background pressure levels in the instrument. The noise in the baseline was generated within the preamplifier. The presence of a peak can usually be recognized when the area of the peak is only 2% of the area of the peak of N_2 (typically the largest peak). The envelope of the 117 spectra as well as measurements of mole fractions of the components of the test gas and driver gases for this run are shown in Fig. 3. The origin of the time axis in Fig. 3a is arbitrary, whereas in Figs. 3b and 3c the time is measured from the rise in pitot pressure at the start of the test flow, an event which occurred at around 0.4 ms in Fig. 3a. Mole fractions are obtained from the concentrations relative to nitrogen by dividing by the sum of the relative concentrations for all species present. The possible presence of NO has been included in the N_2 measurement, since these peaks are inseparable. The test gas measurements are uncalibrated, but the driver gas measurements are calibrated using peak sizes from runs with test gas mixtures of He-N_2 and Ar-N_2 at similar conditions. The

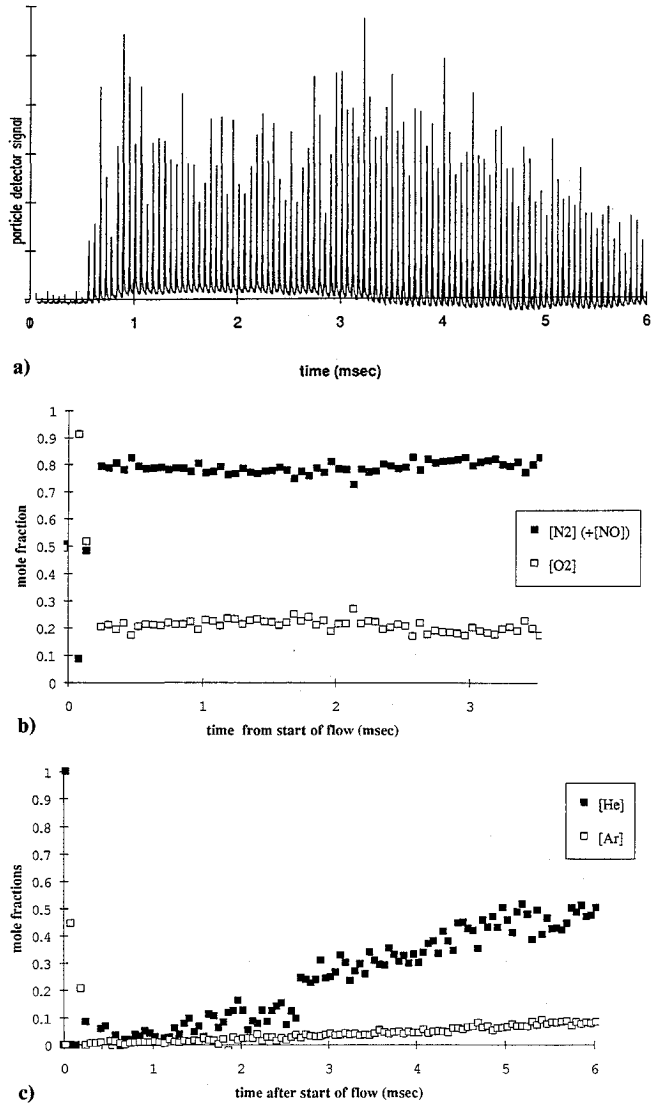

Fig. 3 Concentration measurements from an air test flow at 9-MJ/kg enthalpy: a) envelope of 117 spectra, b) mole fractions of the components of the test gas in the test flow, and c) mole fractions of the components of driver gas.

composition of the driver gas was known to be 15% Ar-85% He. The independently calibrated measurements of relative concentration arrived at the same ratio. The errors in each driver gas concentration data point are 5% absolute.

The instrument had a turn around time of 1.5 h when all went well. Some difficulty was experienced with loss of signal in the higher density flows. These often caused arcing and loss of electric potentials in the ionizer. Some success at overcoming this was found with a temporary electrostatic filter ahead of the third skimmer, indicating that charged particles in the flow were responsible. The tungsten filament and electronics did not suffer overly from the tunnel environment. Vibration did not have any effect, and the three skimmers were not physically degraded by the flow.

Conclusions

A time-of-flight mass spectrometer has been coupled with a compact sampling system to measure species concentrations in hypersonic flows produced by an impulse facility. The ability to detect molecular species present at levels of only 2% by number has been shown. The current limitation on detection is the background noise generated in the signal preamplifier, which leaves the possibility of a more sensitive instrument. The limitations on measurement are the ability to resolve the peaks, the knowledge of the ionization cross section, and the ability to calibrate for gas dynamic

mass separation of disparate mass particles. When these problems are minimized, the error can be 5% for relative concentrations of major species. This is the same level of accuracy that can be achieved by most shock tunnel instrumentation and is superior to other methods of species concentration measurements. At a cost much less than that of most optical systems, the time-of-flight mass spectrometer is a viable addition to the range of diagnostic tools for short duration aerodynamic testing.

Acknowledgments

The authors wish to acknowledge the support received from The Australian Research Council and through NASA Grant NAGW-674.

References

[1]Stalker, R. J., and Crane, K. C., "Driver Gas Contamination in a High Enthalpy Reflected Shock Tunnel," *AIAA Journal*, Vol. 16, No. 3, 1978, pp. 277, 278.

[2]Crane, K. C. A., and Stalker, R. J., "Mass-Spectrometric Analysis of Hypersonic Flows," *Journal of Physics D*, Vol. 10, 1977, pp. 679–685.

[3]Jacobs, P. A., "Quasi-One-Dimensional Modeling of Free-Piston Shock Tunnels," AIAA Paper 93-0352, Jan. 1993.

[4]Kantrowitz, A., and Grey, J., "A High Intensity Source for the Molecular Beam. Pt. 1. Theoretical," *Review of Scientific Instruments*, Vol. 22, No. 5, 1951, pp. 328–332.

[5]Becker, E. W., and Bier, K., "Die Erzeugung eines intensiven, teilweise monochromatisierten Wasserstoff-Molekularstrahles mit einer Laval-Düse," *Zeitschrift fuer Naturforsching*, Vol. 9a, Aug. 1954, pp. 975–986.

[6]Skinner, G. T., "Molecular Beam for the Study of High-Temperature-Gas Collision Processes," *Physics of Fluids*, Vol. 4, 1961, pp. 1172–1176.

[7]Bird, G. A., "Transition Regime Behaviour of Supersonic Skimmers," *Physics of Fluids*, Vol. 19, No. 10, 1976, pp. 1486–1491.

[8]Sebacher, D. I., "Diffusive Separation in Shock Waves and Freejets of Nitrogen-Helium Mixtures," *AIAA Journal*, Vol. 6, No. 1, 1968, pp. 51–58.

[9]Sherman, F. S., "Hydrodynamical Theory of Diffusive Separation of Mixtures in a Free Jet," *Physics of Fluids*, Vol. 8, No. 5, 1965, pp. 773–779.

[10]Fenn, J. B., and Anderson, J. B., "Background and Sampling Effects in Free Jet Studies by Molecular Beam Measurements," *Proceedings of 4th International Symposium on Rarefied Gas Dynamics* (Toronto, Canada), Academic Press, New York, 1966, pp. 311–330.

[11]Wiley, W. C., and McLaren, I. H., "Time-of-Flight Mass Spectrometer with Improved Resolution," *Review of Scientific Instruments*, Vol. 26, No. 12, 1955, pp. 1150–1157.

Lamination Parameters for Reissner-Mindlin Plates

Joachim L. Grenestedt*
Royal Institute of Technology, Stockholm S-100 44, Sweden

Introduction

TSAI and Pagano[1] introduced 12 parameters—called lamination parameters—to express plate stiffnesses of laminated composite Kirchhoff plates. These parameters considerably simplify design and optimization of thin composites compared with using layup angles and thicknesses of discrete plies in a laminate. A layup gives a unique set of lamination parameters, but many layups might give the same set of lamination parameters. The lamination parameters fully describe the plate stiffnesses, and they can therefore be used as design variables for structural design and optimization. Examples can be found in Miki[2,3] and Grenestedt.[4] By using these parameters rather than ply layup angles and thicknesses, the major problem of local optima during optimization is often overcome. The stiffnesses are linear in the lamination parameters, the range of the lamination parameters is convex (see Grenestedt and Gudmundson[5]), and a number of optimization problems therefore become convex (see Svanberg[6]). Further, all physically possible layups are simply included in the analysis with just a small number of parameters. The purpose of the current Note is to derive lamination parameters for kinematically nonlinear small strain, medium rotation shear deformable Reissner-Mindlin type[7,8] plates. For the sake of completeness, the Reissner-Mindlin equations as well as the Tsai and Pagano lamination parameters are derived in the following sections.

Governing Equations of Laminated Reissner-Mindlin Type Plates

In the following, Einstein's summation convention is used. Greek indices run from 1 to 2 and Latin from 1 to 3. Cartesian Lagrangian coordinates x_i with the x_3 axis perpendicular to the undeformed plate middle surface are introduced. The displacement field is assumed to be

$$\begin{aligned} u_\alpha(x_1, x_2, x_3) &= \bar{u}_\alpha(x_1, x_2) + x_3\theta_\alpha(x_1, x_2) \\ u_3(x_1, x_2, x_3) &= \bar{u}_3(x_1, x_2) \end{aligned} \tag{1}$$

where u_i are displacement components, and $\bar{u}_i$ are middle surface displacement components. The Green-Lagrange strain tensor is, when gradients of in-plane displacements are assumed small,

$$e_{\alpha\beta} = \overset{0}{e}_{\alpha\beta} + x_3\kappa_{\alpha\beta} \tag{2}$$

where

$$\begin{aligned} \overset{0}{e}_{\alpha\beta} &= (\bar{u}_{\alpha,\beta} + \bar{u}_{\beta,\alpha} + \bar{u}_{3,\alpha}\bar{u}_{3,\beta})/2 \\ \kappa_{\alpha\beta} &= (\theta_{\alpha,\beta} + \theta_{\beta,\alpha})/2 \end{aligned} \tag{3}$$

and

$$e_{\alpha 3} = (\bar{u}_{3,\alpha} + \theta_\alpha)/2 \tag{4}$$

As constitutive relation, elastic behavior with a strain energy per unit plate surface area

$$W\left(\overset{0}{e}_{\alpha\beta}, e_{\alpha 3}, \kappa_{\alpha\beta}\right) \tag{5}$$

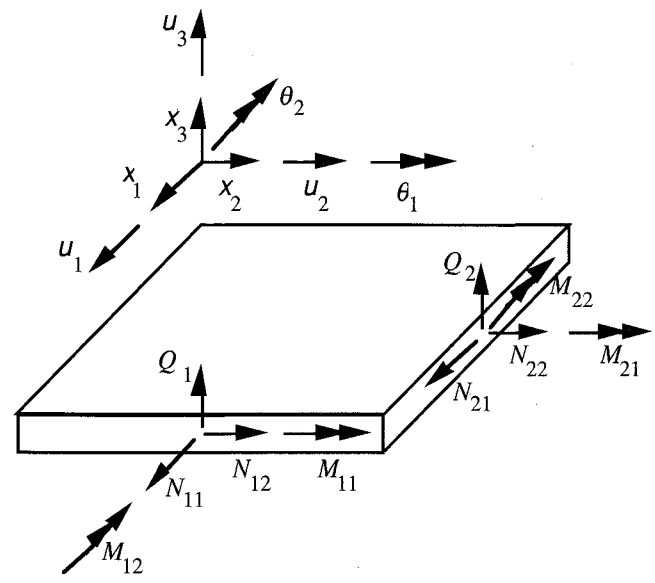

Fig. 1 Notation and sign conventions for the plate variables.

Received Jan. 19, 1994; revision received May 9, 1994; accepted for publication May 9, 1994.

*Senior Research Engineer, Department of Lightweight Structures. Member AIAA.